

# Metabolic positron-emission tomography/magnetic resonance imaging in primary progressive aphasia and frontotemporal lobar degeneration subtypes: Reassessment of expected [<sup>18</sup>F]-fluorodeoxyglucose uptake patterns

## ABSTRACT

Clinical assessment of frontotemporal lobar degeneration (FTLD)/primary progressive aphasia (PPA) patients is challenging, given that common cognitive assessments rely extensively on language. Since asymmetry in neuroimaging biomarkers is often described as a central finding in these patients, our study evaluated [<sup>18</sup>F]-fluorodeoxyglucose (FDG) uptake patterns in patients meeting clinical and imaging criteria for FTLD, with emphasis on PPA. Fifty-one subjects underwent brain [<sup>18</sup>F]-FDG positron-emission tomography/magnetic resonance imaging (PET/MRI) as part of their routine clinical workup for dementia and neurodegenerative disease. Images were obtained using a Siemens Biograph mMR integrated 3T PET/MRI scanner. PET surface maps and fusion fluid-attenuated inversion recovery-PET images were generated utilizing MIMneuro software. Two board-certified neuroradiologists and one nuclear medicine physician blinded to patient history classified each FTLD/PPA subtype and assessed for left- versus right-side dominant hypometabolism. Qualitative and semiquantitative assessment demonstrated 18 cases of PPA, 16 behavioral variant frontotemporal dementia (bvFTD), 12 corticobasal degeneration, and 5 progressive supranuclear palsy. Among the 18 PPA subjects (11 svPPA, 5 lvPPA, and 2 agPPA), 12 (67%) demonstrated left-dominant hypometabolism and 6 (33%) right-dominant hypometabolism. While existing literature stresses left-dominant hypometabolism as a key imaging feature in the PPA subtypes, a third of our cases demonstrated right-dominant hypometabolism, suggesting that emphasis should be placed on the functionality of specific brain regions affected, rather than left versus right sidedness of hypometabolism patterns.

**Keywords:** [<sup>18</sup>F]-fluorodeoxyglucose, frontotemporal lobar degeneration, hybrid neuroimaging, positron emission tomography/magnetic resonance imaging, primary progressive aphasia

## INTRODUCTION

With an aging population, the diagnosis of dementia is becoming increasingly important. This can be challenging for clinicians, especially in the early stages of the disease, and may often be confounded by patients with higher education levels, comorbid conditions, and the use of certain medications limiting clinical assessment.<sup>[1]</sup> Therefore, novel imaging biomarkers are becoming increasingly important in the clinical workup of patients presenting with cognitive impairment.

Primary progressive aphasia (PPA) is a relatively uncommon syndrome primarily affecting language,

**ANA M. FRANCESCHI, KIYON NASER-TAVAKOLIAN<sup>1</sup>,  
MICHAEL CLIFTON<sup>1</sup>, LEV BANGIYEV<sup>1</sup>,  
GIUSEPPE CRUCIATA<sup>1</sup>, SEAN CLOUSTON<sup>2</sup>,  
DINKO FRANCESCHI<sup>1</sup>**

Department of Radiology, Neuroradiology Section, Northwell Health/Donald and Barbara Zucker School of Medicine, Manhasset, Departments of <sup>1</sup>Radiology and Family and <sup>2</sup>Population and Preventive Medicine, SUNY Stony Brook, Stony Brook, NY, USA

**Address for correspondence:** Dr. Ana M. Franceschi, Northwell Health, Department of Radiology, 300 Community Drive, Manhasset, NY, 11030-3816 USA.  
E-mail: afranceschi@northwell.edu


**Submitted:** 13-Oct-2020, **Revised:** 18-Nov-2020,  
**Accepted:** 19-Nov-2020, **Published:** 26-May-2021

This is an open access journal, and articles are distributed under the terms of the Creative Commons Attribution-NonCommercial-ShareAlike 4.0 License, which allows others to remix, tweak, and build upon the work non-commercially, as long as appropriate credit is given and the new creations are licensed under the identical terms.

**For reprints contact:** WKHLRPMedknow\_reprints@wolterskluwer.com

**How to cite this article:** Franceschi AM, Naser-Tavakolian K, Clifton M, Bangiyev L, Cruciata G, Clouston S, *et al.* Metabolic positron-emission tomography/magnetic resonance imaging in primary progressive aphasia and frontotemporal lobar degeneration subtypes: Reassessment of expected [<sup>18</sup>F]-fluorodeoxyglucose uptake patterns. *World J Nucl Med* 2021;20:294-304.

### Access this article online

<b>Website:</b> www.wjnm.org	<b>Quick Response Code</b> 
<b>DOI:</b> 10.4103/wjnm.wjnm_137_20	

which is categorized under the umbrella term of frontotemporal lobar degeneration (FTLD).<sup>[2-5]</sup> Specifically, the clinical diagnosis of PPA requires that a progressive language impairment be the primary cognitive deficit for approximately 2 years after symptom onset, with minimal difficulty in other cognitive functions. Three subtypes of PPA are currently recognized in the literature: semantic variant (svPPA), logopenic variant (lvPPA), and agrammatic variant (agPPA), also known as progressive nonfluent aphasia. The characteristic clinical features of svPPA include anomia and single-word comprehension deficits; lvPPA patients demonstrate deficits in word retrieval and sentence repetition, while agPPA presents with agrammatism in language production and effortful speech.<sup>[4,5]</sup>

Pathologic studies have demonstrated the PPA syndromes to be associated with different abnormal cellular proteins, not in perfect association with the three PPA subtypes, resulting in the significant overlap. For example, the microtubule-associated protein tau has been shown to aggregate in its abnormal hyperphosphorylated form resulting in neurofibrillary tangles which are the underlying histopathologic hallmark in various dementia subtypes, including Alzheimer's disease (AD), chronic traumatic encephalopathy, and even some cases of PPA and related FTLD variants.<sup>[6-9]</sup> Specifically, different splicing of the three exons in tau yields three different isoforms of abnormal tau deposition: tau with 4 microtubule-binding domains (4R tau) associated with agPPA; tau with 3 microtubule-binding domains (3R tau); and tau with almost equal amounts of both (3R+4R tau) associated with lvPPA. In contrast, the svPPA variant is rarely associated with tau isoforms and is more commonly associated with TAR DNA-binding protein 43.<sup>[10]</sup>

In our current work, we reassess the expected metabolic neuroimaging features in patients with clinical concern for PPA and related FTLD variants. Prior reports have emphasized the overall left-sided predominance of hypometabolism patterns in all PPA subtypes.<sup>[11-17]</sup> However, clinical experience among the authors has not fully validated the utility of prior generalizations in the context of high-resolution positron-emission tomography/magnetic resonance (PET/MR) scanners in conjunction with new semiquantitative software. This study therefore employed hybrid [<sup>18</sup>F]-fluorodeoxyglucose (FDG) PET/magnetic resonance imaging (MRI) to evaluate for characteristic patterns of decreased FDG uptake and cortical atrophy in these patients, with a particular focus on left- versus right-sided dominant hypometabolism.

## MATERIALS AND METHODS

All subjects underwent brain [<sup>18</sup>F]-FDG PET/MRI as part of their routine clinical care.

This HIPAA (Health Insurance Portability and Accountability Act) compliant study received a local institutional review board approval. Written informed consent was waived due to the retrospective nature of this study.

Before imaging, an injection of approximately 5 mCi (185 MBq) of FDG was given intravenously. All subjects had fasting blood glucose level <150 mg/dL and were placed in a dimly lit room, with their eyes open. After 40 min of uptake, the subject was positioned for brain imaging in a Siemens mMR 3T PET/MRI (Siemens Healthcare, Erlangen, Germany) scanner with a standard 12-channel head coil. A dual-echo T1-weighted gradient-recalled echo sequence was performed to acquire the MRI attenuation-correction map based on a Dixon segmentation (air, fat, soft tissue, and lungs). Further postprocessing of PET data was performed utilizing MIMneuro version 6.9.5 (MIM Software, Inc., Cleveland, Ohio, USA). Images were spatially normalized to a standard brain template using a process of image translation, rotation, and scaling followed by an iterative landmark matching and thin-plate deformable registration technique. Three-dimensional (3D) stereotactic surface projections were created. The PET data were reconstructed with an iterative 3D ordinary Poisson ordered subsets expectation-maximization algorithm at 3 iterations and 21 subsets and with a 4-mm Gaussian postreconstruction image filter. PET image matrix size was 344 mm × 344 mm × 127 mm, and transaxial voxel dimensions were 1.04 mm × 1.04 mm with a thickness of 2.03 mm. PET data were acquired for a total of 20 min.

MRI data included images from the skull vertex to the foramen magnum. Standard high-resolution 3D sagittal MPRAGE and 3D fluid-attenuated inversion recovery (FLAIR) sequences were used for brain anatomy. Afterward, routine diagnostic MRI sequences were performed, while PET data were simultaneously obtained, as follows:

The 3D FLAIR fat-suppressed sagittal images were obtained using the following parameters: repetition time/echo time/inversion time (TI) of 5000 ms/402 ms/1800 ms; field of view (FOV) of 250 mm; voxel size 0.9 mm × 0.9 mm × 0.9 mm; slice thickness 0.9 mm; and an acquisition time of 7 min. The 3D sagittal MPRAGE sequence was obtained using a repetition time/echo time/TI of 1700 ms/2.44 ms/841 ms; a FOV of 250 mm; voxel size; 1.0 mm × 1.0 mm × 1.0 mm; slice thickness 1.0 mm; flip angle of 9°; and acquisition time of 3 min and

58 s. The MR-based attenuation corrected PET sequence was obtained using a repetition time/echo time 1 and echo time 2 of 3.6 ms/1.23 ms and 2.46 ms; FOV of 500 mm; voxel size 4.2 mm × 2.6 mm × 3.1 mm; slice thickness 3.12 mm; flip angle of 10°; and acquisition time of 19 s. The DTI sequence was obtained using the following parameters: repetition time/echo time 5600 ms/90 ms; FOV of 250 mm; voxel size 2.0 mm × 2.0 mm × 4.0 mm; slice thickness 4 mm; delay of 0 ms; and an acquisition time of 3 min and 10 s. The T2 TSE in the axial plane was obtained using the following parameters: repetition time/echo time of 4000 ms/96.0 ms; FOV 230 mm; voxel size 0.8 mm × 0.7 mm × 3.0 mm; slice thickness 3.0 mm with 0 ms of delay flip angle of 150°; and acquisition time of 1 min and 12 s. Diffusion images were obtained using repetition time/echo time of 7500 ms/92.0 ms; FOV 240 mm; voxel size 1.5 mm × 1.5 mm × 4.0 mm; slice thickness 4.0 mm with 0 ms of delay; and acquisition time of 2 min and 8 s.

### Image analysis

Two neuroradiology fellowship-trained board-certified radiologists with dedicated brain PET/MRI clinical and research experience independently reviewed the fused PET/MRI sequences and classified each case according to FTLD/PPA subtype of neurodegenerative disease. Subjects were categorized into FTLD variants on the basis of imaging and clinical criteria, as follows: PPA (semantic, logopenic, or agrammatic variant);<sup>[3-5]</sup> behavioral variant frontotemporal dementia (bvFTD);<sup>[2,18]</sup> corticobasal degeneration (CBD);<sup>[19-21]</sup> and progressive supranuclear palsy (PSP).<sup>[2,22,23]</sup> Specifically, we assessed for pronounced hypometabolism in the anterior temporal regions for svPPA; lateral parietal and temporal regions for lvPPA; perisylvian and posterior frontal regions for agPPA; frontal regions and anterior cingulate gyrus for bvFTD; single hemisphere with ipsilateral basal ganglia and thalamus for CBD; and posterior frontal regions, anterior cingulate gyrus, basal ganglia, and midbrain for PSP.

Along with qualitative assessment, 3D MPRAGE: High-resolution three-dimensional magnetization-prepared rapid acquisition with gradient echo sequence MR image data were additionally evaluated by NeuroQuant (2019 CorTechs Labs, Inc., San Diego, California, USA) for quantitative volumetric analysis. NeuroQuant is an FDA-cleared software that analyzes the intracranial volume and comparing these volumes to a normative database. NeuroQuant compares lobar and sublobar cortical volumes to their standardized database, which are adjusted for age, sex, and volume status. Regions of parenchymal volume loss >2 standard deviations from normal controls in the standardized atlas were flagged as abnormal. Quantitative percentages were assigned to lobar and sublobar areas to quantify the extent of parenchymal

volume loss. NeuroQuant software provides semiquantitative data regarding the aforementioned variables and does not provide a dementia diagnosis.

One nuclear medicine physician with 25 years of experience in brain PET imaging reviewed the PET portion of the study with additional cortical surface map reconstructions (qualitative assessment) and semiquantitative Z-score analysis of brain hypometabolism utilizing MIMneuro software. MIMneuro software runs a region-based analysis which calculates Z-scores (number of standard deviations from the mean) and asymmetry measurements for individual brain regions defined by the Single Brain Atlas and MIM Probabilistic anatomical atlas to provide semiquantitative analysis of brain hypometabolism. As per the manufacturer, the Single Brain Atlas and MIM Probabilistic anatomical atlas are composed of 43 individuals (19 females and 24 males) with an age range of 41–80 years. The distribution of the normal age-based atlas is as followed: six subjects aged 40–49 years, eight subjects aged 50–59 years, 14 subjects aged 60–69 years, 14 subjects aged 70–79 years, and one subject with age between 80 and 89 years. The mean age and standard deviation of these 43 individuals are 63.8 ± 9.98 years. The automated Z-scores are calculated by comparing the patient to the selected age-matched set of normal controls (within 5 years of the patient's age). MIMneuro software provides semiquantitative Z-score analysis regarding the aforementioned variables and does not provide dementia diagnosis.

All three readers then separately scored the supratentorial brain parenchymal FDG uptake, analyzing the images for left versus right predominant hypometabolism. The scoring was as follows: Symmetrical, asymmetrical L > R, or asymmetrical R > L hypometabolism. Any discrepancy was resolved by consensus review among the readers.

### RESULTS

Fifty one subjects underwent hybrid [<sup>18</sup>F]-FDG PET/MRI as part of their routine clinical workup for underlying neurodegenerative disease and were ultimately diagnosed with FTLD/PPA on the basis of neurologic workup including cognitive testing and imaging findings, of which 18 subjects with PPA (11 svPPA, 5 lvPPA, and 2 agPPA), 16 subjects with bvFTD, 12 with CBD, and 5 with PSP.

Clinical and demographic data for the FTLD/PPA subtypes are outlined in Table 1.

Relevant PET/MRI findings are summarized in Table 2.

**Table 1: Clinical and demographic subject data**

Disease	Number of patients by sex	Average age	Average MoCA score	Common presenting symptoms	Common findings on neurocognitive testing
Semantic PPA	6 male 5 female	73.8	23	Progressive memory loss Impaired word recall Impaired concentration	Impaired semantic fluency Impaired delayed recall Impaired memory Impaired executive functioning
Logopenic PPA	3 male 2 female	74.8	-	Short-term memory loss Impaired concentration Expressive aphasia	Impaired delayed recall Impaired new learning Impaired executive functioning Impaired memory
Agrammatic PPA	1 male 1 female	76.5	-	Language difficulties Difficulty remembering the correct word	Impaired language functioning Impaired reading comprehension Impaired new learning Slow verbal fluency Impaired complex attention tasks
FTD – BV	8 male 8 female	71.8	-	Short term memory loss Difficulty with ADL's and IADL's Behavioral changes and mood swings	Decreased higher-order reasoning and memory Impaired short term and delayed recall Attention dysfunction Impaired executive functioning
FTD – CBD	3 male 9 female	74.6	21.4	Progressive memory loss Unilateral ataxia and tremor Impaired rapid alternating hand movements	Impaired visuospatial Impaired executive functioning Impaired delayed recall
FTD – PSP	2 male 3 female	72.6	-	Memory problems Slower movements Involuntary movements Balance difficulties	Impaired executive functioning Slow speech Bradykinesia

PPA: Primary progressive aphasia, FTD: Frontotemporal dementia, BV: Behavioral variant, CBD: Corticobasal degeneration, PSP: Progressive supranuclear palsy, ADL's: Activities of daily livings, IADL's: Instrumental ADL's, MoCA: Montreal cognitive assessment

**Table 2: Summary of [18F] FDG-PET and MRI findings**

Disease	PET hypometabolism	MRI volume loss
Semantic PPA	Anterior temporal lobes To a lesser degree, frontal lobes Normal FDG uptake in precuneus and posterior cingulate gyrus	Temporal pole Amygdala Parahippocampal gyri and entorhinal cortex Fusiform gyrus Inferior and middle temporal gyri
Logopenic PPA	Lateral parietal and posterior temporal regions Precuneus and posterior cingulate gyrus	Lateral parietal lobe Precuneus Angular and supramarginal gyri Posterior temporal lobe Superior temporal gyrus
Agrammatic PPA	Posterior frontal and fronto-insular regions Perisylvian distribution	Insular cortex Frontal operculum Inferior frontal gyri (pars opercularis and pars orbitalis)
FTD – BV	Frontal lobes To a lesser degree, temporal lobes Anterior cingulate gyrus	Frontal and anterior temporal lobes Orbitofrontal cortex Caudate head
FTD – CBD	Single cerebral hemisphere Ipsilateral basal ganglia and thalamus Sensorimotor cortex	Superior parietal lobule Peri-rolandic cortex (precentral and postcentral gyri) Corpus callosum Basal ganglia
FTD – PSP	Posterior frontal regions Anterior cingulate gyrus Basal ganglia and midbrain	Brainstem atrophy Reduced midbrain to pons area ratio Flattening of the superior aspect of the midbrain Reduced midbrain AP diameter

PPA: Primary progressive aphasia, FTD: Frontotemporal dementia, BV: Behavioral variant, CBD: Corticobasal degeneration, PSP: Progressive supranuclear palsy, PET: Positron emission tomography, FDG: Fluorodeoxyglucose, AP: Anteroposterior, MRI: Magnetic resonance imaging

Of the 18 subjects meeting clinical and imaging criteria for PPA,<sup>[3-5]</sup> 11 (6 male, 5 female; age range: 57–87 years) demonstrated pronounced anterior temporal hypometabolism consistent with svPPA. Five cases (3 male, 2 female; age range:

68–83 years) demonstrated predominantly lateral parietal and posterior temporal hypometabolism also involving the precuneus and posterior cingulate gyrus compatible with underlying lvPPA and 2 subjects (1 male, 1 female; age

74 and 79 years, respectively) demonstrated perisylvian hypometabolism as well as decreased FDG uptake in the posterior frontal regions including in the frontal operculum compatible with agPPA.

Among these 18 subjects with underlying PPA, 12 (67%) demonstrated left-predominant pattern and 6 (33%) right-predominant pattern of decreased FDG uptake.

Of the 11 subjects with svPPA, 8 (73%) had left temporal pole predominant hypometabolism, while 3 (27%) demonstrated most pronounced findings in the right temporal pole.

Figure 1a-d demonstrates a patient with PET/MRI findings suggestive of svPPA. Cortical surface maps [Figure 1a] demonstrated markedly abnormal FDG distribution pattern with marked decreased radiotracer uptake in the bilateral temporal lobes and specifically in the temporal poles bilaterally, findings more pronounced on the right side. There is also moderate hypometabolism in the frontal and mild-to-moderate hypometabolism in the parietal lobes (right greater than left), as well as in the bilateral anterior cingulate gyrus. The axial PET maps provide further insight into the anatomy and distribution of the hypometabolism as well as cortical volume loss, with striking decreased tracer uptake in the right temporal pole [Figure 1b]. Findings were confirmed on Z-score overlay on PET cortical surface maps [Figure 1c]. The tabular output of semiquantitative analysis using the Z-scores calculated in comparison to age-matched normal controls [Figure 1d] for this patient revealed decreased values in the temporal lobes, frontal regions, and also in the right anterior cingulate gyrus.

Of the five patients with underlying lvPPA, 3 cases (60%) demonstrated left lateral parietal and posterior temporal hypometabolism, while 2 (40%) had strongly affected the right lateral parietotemporal region, including the precuneus and posterior cingulate.

Figure 2a-d demonstrates a patient with PET/MRI findings suggestive of lvPPA. Cortical surface maps [Figure 2a] demonstrated decreased tracer uptake in the right frontal, parietal, and temporal regions, with most pronounced hypometabolism in the right lateral parietotemporal region, and also moderately decreased FDG uptake in the left frontal lobe and moderate-to-severe decreased FDG uptake in the left lateral parietotemporal region. These findings are confirmed on fusion axial images as well as on the Z-score overlays (Figure 2b-c), which provide further insight into the anatomy and distribution of hypometabolism. Semiquantitative analysis results with Z-scores calculated in comparison to

age-matched normal controls in tabular output [Figure 2d] for this patient revealed decreased values in the right temporal, parietal, and frontal lobes, as well as in the left middle and inferior temporal gyrus. There were also decreased FDG Z-score values in the right precuneus and right posterior cingulate gyrus [Figure 2d], regions typically involved early in patients with underlying Alzheimer's pathology, which is commonly the cause of logopenic PPA.

Finally, of the two subjects with suspected agPPA, one demonstrated left-dominant hypometabolism and the other subject demonstrated symmetric to slightly right-dominant hypometabolism in the perisylvian region, and also involving the posterior frontal regions, frontal operculum, and anterior cingulate gyrus.

Figure 3a-d demonstrates a patient with PET/MRI findings most suggestive of agPPA. Cortical surface PET maps [Figure 3a] demonstrate decreased tracer activity in the posterior frontal lobes and anterior cingulate gyrus, findings slightly more pronounced on the right side. Moderate hypermetabolism is evident, particularly in the right perisylvian region. These findings were confirmed on the fusion PET and FLAIR MRI axial images as well as the Z-score overlays [Figure 3b and c], which provide more insight into the anatomy and distribution of hypometabolism. MIM Z-score tabular output [Figure 3d] used for semiquantitative assessment highlights (slight) right predominance of hypometabolism pattern in comparison to age-matched cognitively normal controls and reveals decreased values in the bilateral frontal lobes, including in the pars opercularis and pars triangularis of the inferior frontal gyrus (Broca's region), and also in the right anterior cingulate gyrus.

Of the 16 subjects meeting clinical and imaging criteria for bvFTD<sup>[2,18]</sup> (8 male, 8 female; average age 72), 12 (75%) demonstrated left-predominant hypometabolism and 3 (19%) demonstrated right-predominant hypometabolism, while one subject had symmetric hypometabolism involving the bilateral frontal lobes, including in the anterior cingulate gyrus, and to a lesser extent in the temporal lobes.

Of the 12 subjects meeting clinical and imaging criteria for CBD<sup>[19-21]</sup> (9 female, 3 male; average age 74.3), 6 (50%) had left and 4 (33%) right asymmetric hypometabolism involving nearly the entire cerebral hemisphere including the ipsilateral basal ganglia and thalamus, while 2 CBD subjects demonstrated a more atypical symmetric pattern of hypometabolism including involvement of the bilateral sensorimotor cortices.

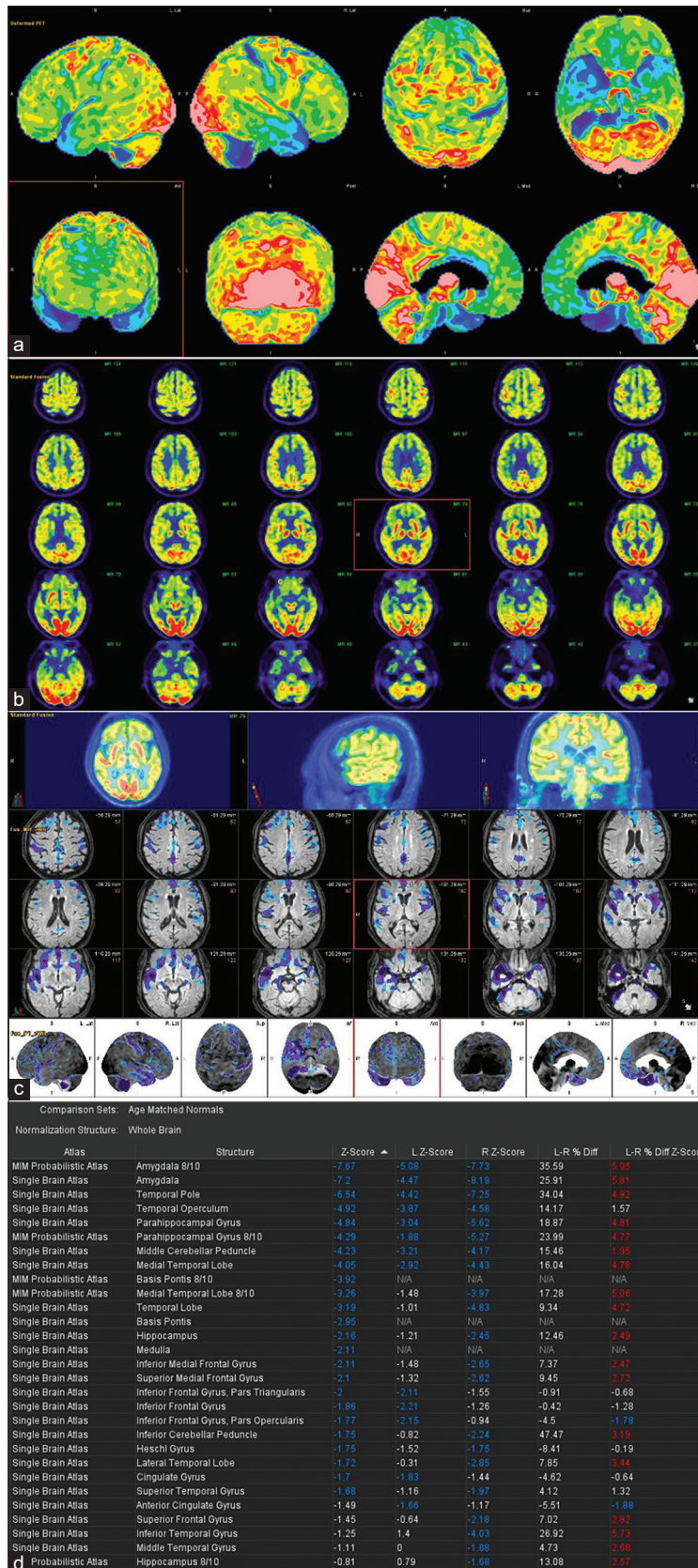


Figure 1: [18F]-fluorodeoxyglucose positron-emission tomography/magnetic resonance imaging findings in a patient with right-dominant semantic variant primary progressive aphasia. (a) [18F]-fluorodeoxyglucose-positron emission tomography cortical surface maps. (b) Fusion [18F]-fluorodeoxyglucose positron emission tomography and fluid-attenuated inversion recovery magnetic resonance imaging axial images. (c) Z-score overlay on cortical surface maps. (d) MIM Z score tabular output

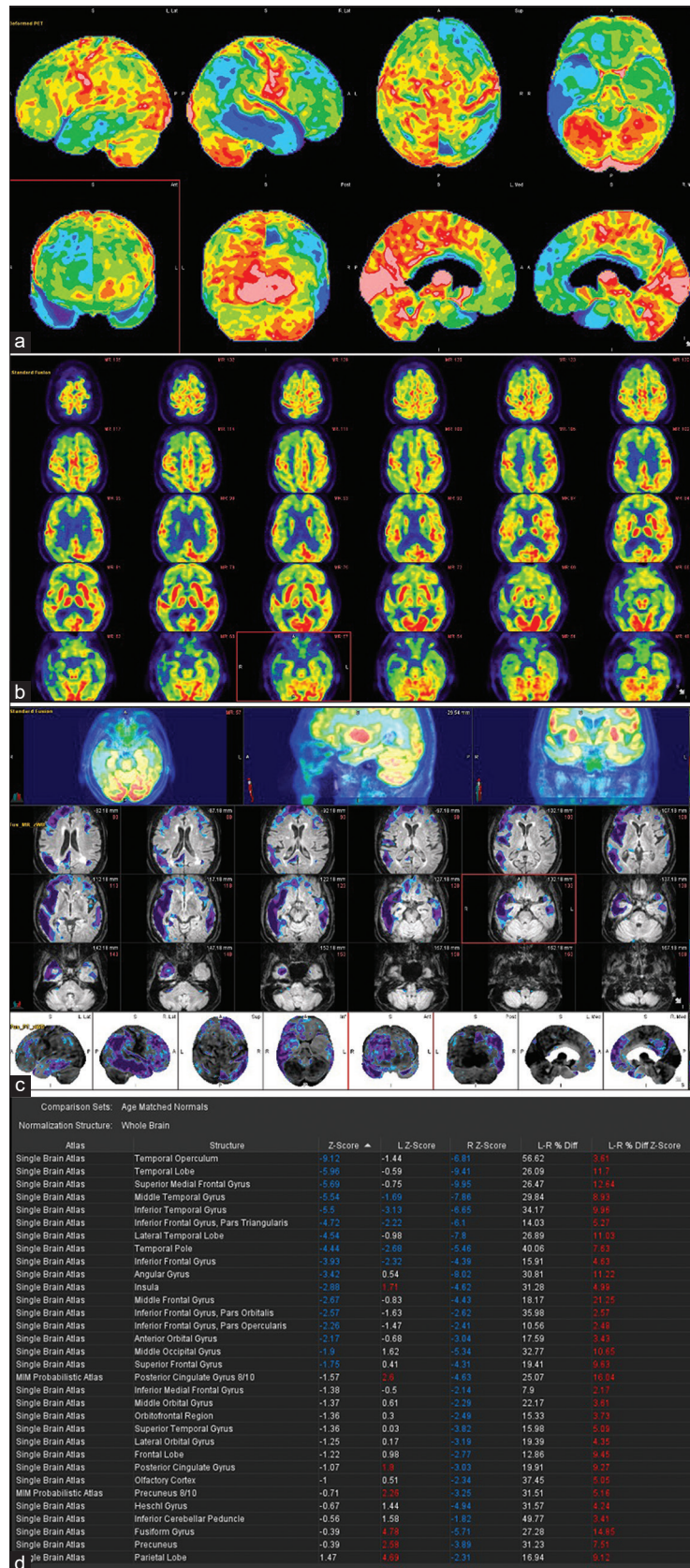


Figure 2: [<sup>18</sup>F]-fluorodeoxyglucose positron emission tomography/magnetic resonance imaging findings in a patient with right-dominant logopenic variant primary progressive aphasia. (a) [<sup>18</sup>F]-fluorodeoxyglucose- positron-emission tomography cortical surface maps. (b) Fusion [<sup>18</sup>F]-fluorodeoxyglucose positron emission tomography and fluid-attenuated inversion recovery magnetic resonance imaging axial images. (c) Z-score overlay on cortical surface maps. (d) MIM Z score tabular output

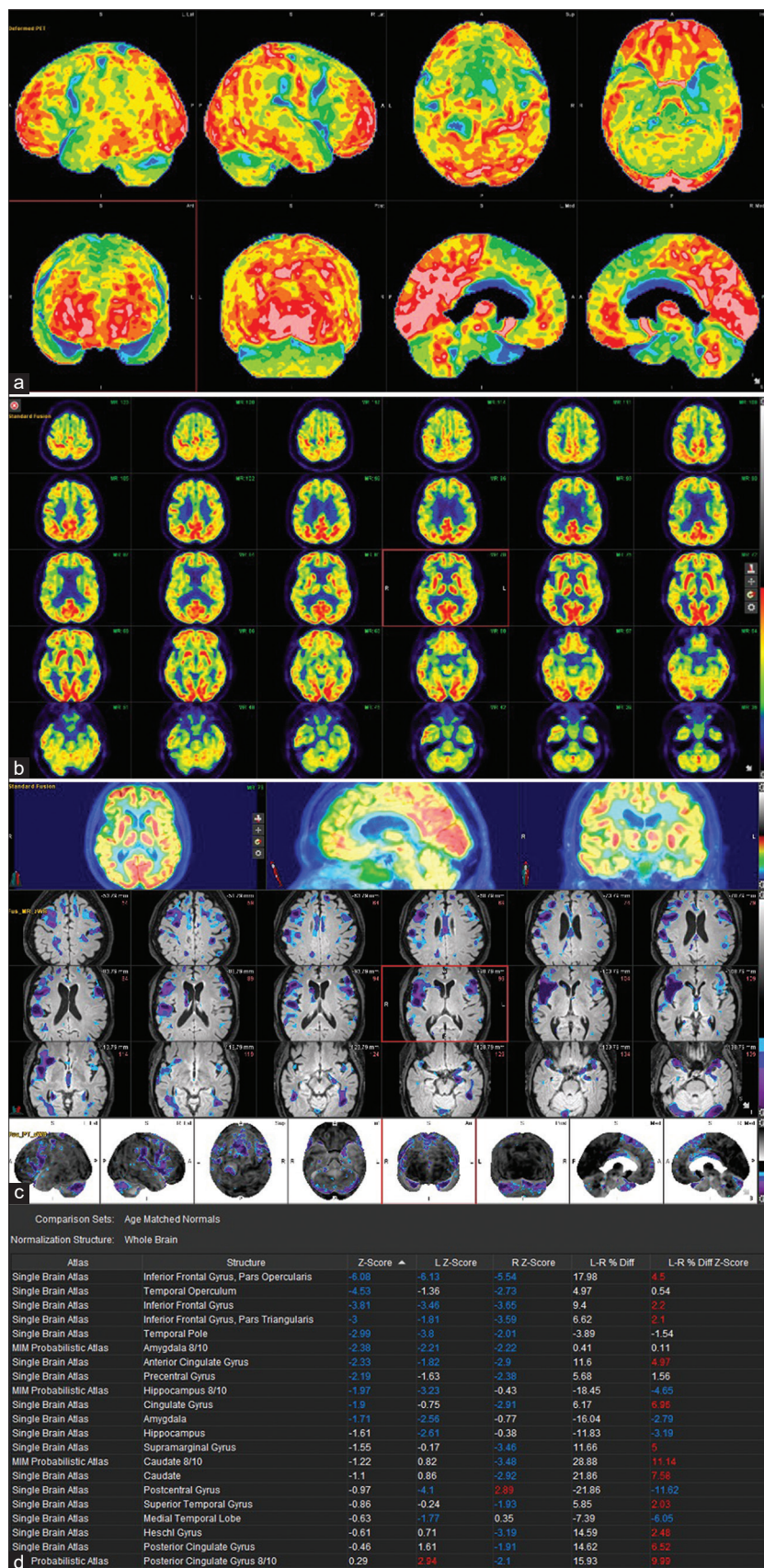


Figure 3: [<sup>18</sup>F]-fluorodeoxyglucose positron emission tomography/magnetic resonance imaging findings in a patient with right-dominant agrammatic variant primary progressive aphasia. (a) Cortical surface map. (b) Fusion [<sup>18</sup>F]-fluorodeoxyglucose positron-emission tomography and fluid-attenuated inversion recovery axial magnetic resonance imaging axial images. (c): Z-score overlay on cortical surface maps. (d) MIM Z score tabular output



Among the five subjects meeting clinical and imaging criteria for PSP<sup>[2,22,23]</sup> (three female, two male; average age 72.6), three (60%) demonstrated left-dominant hypometabolism, one right predominant hypometabolism, Among the 5 subjects meeting clinical and imaging criteria for PSP [2, 22-23] (3 female, 2 male; average age 72.6), 3 subjects (60%) demonstrated left dominant hypometabolism, one subject demonstrated right predominant hypometabolism; and one subject had a symmetric pattern of decreased FDG uptake in the bilateral posterior frontal lobes and anterior cingulate gyrus, basal ganglia and midbrain.

It was noted that PET image interpretation was performed both by visual assessment and semiquantitative analysis, with the results in concordance across all subjects. Patterns of MRI volume loss and regional atrophy correlated with PET findings, including the described asymmetry in our patient cohort.

## DISCUSSION

Our study addresses the metabolic and structural hybrid neuroimaging evaluation of cognitively impaired patients with suspected FTLD, and specifically, presenting clinically with language-predominant symptomatology concerning for PPA, who underwent brain [<sup>18</sup>F]-FDG PET/MRI as part of their routine clinical dementia workup.

FTLD consists of a group of clinically and pathologically heterogeneous neurodegenerative disorders with varied clinical features, but, overlapping underlying pathologic and genetic etiologies, and also, neuroimaging findings which can make accurate diagnosis difficult.<sup>[2,24-26]</sup> In particular, PPA patients typically present with vague and oftentimes nonspecific language-related deficits, which may be challenging to accurately diagnose clinically, particularly in the early stages of disease when potential treatment and management planning can have the most impact.<sup>[3-5]</sup> Overall, an accurate diagnosis of the underlying neurodegenerative process is imperative due to the potentially devastating consequences for the patients and their families, especially since the appropriate selection of disease-modifying treatments, particularly in the setting of emerging dementia therapeutics, can significantly vary depending on the cause and subtype of the underlying neurodegenerative process.<sup>[1,27]</sup> To this end, further work is needed on the development of multimodal diagnostic methods, combining neuro- and molecular imaging findings, neuropsychological testing, cerebrospinal fluid, and genetic biomarkers.

Regarding metabolic imaging findings, prior FDG-PET studies in the literature have suggested that careful attention to

affected brain regions and their functionality may not only provide a more accurate diagnosis but also allow us to differentiate among the FTLD pathologies, including the PPA subtypes, given that specific patterns of hypometabolism correspond to known regions of brain atrophy on gross pathology, and matching clinical syndromes.<sup>[11-17]</sup>

For example, patients with svPPA classically demonstrate prominent anterior temporal hypometabolism (left greater than right), while patients with lvPPA typically show greatest reductions in FDG uptake in the left parietal and posterolateral temporal lobes, including the precuneus and posterior cingulate gyrus. Finally, patients with agPPA demonstrate asymmetric involvement of the left perisylvian and posterior frontal regions, including the frontal operculum.<sup>[13-17]</sup> Furthermore, areas of atrophy and hypometabolism in the three PPA variants have previously been described in the literature as overwhelmingly left sided and highlighted as a key distinguishing imaging feature from other neurodegenerative processes. In fact, sparing of the right temporoparietal cortex has been used to differentiate patients with logopenic PPA (also referred to as language-variant AD due to similarity of underlying histopathologic features), from subjects with classic AD.<sup>[16]</sup> These findings have also been supported by previous quantitative FDG analyses which confirm the premise that regions of greatest metabolic disruption closely match the expected clinical syndromes. For example, patients with lvPPA demonstrate the greatest asymmetry (in favor of left dominant hypometabolism) in the temporoparietal regions of interest (ROIs), patients with agPPA in the left frontal ROIs, and patients with svPPA in the left anterior temporal ROIs. When grouped together, asymmetric left hypometabolism was dominant across the whole cortex, frontal, and anterior temporal ROIs, with a trend toward statistical significance in the temporoparietal ROIs.<sup>[14]</sup>

In our study, the majority of patients presenting with clinical and imaging features of underlying PPA did, in fact, demonstrate the expected left-side predominance of metabolic disruption.<sup>[11-17]</sup> However, this was not a hard rule, and in fact, rather surprisingly a third of our subjects with suspected PPA were noted to have strongly right-side dominant hypometabolism. Therefore, it is evident that much more complex underlying genetic and molecular markers are at play and should be further explored to better explain the metabolic imaging deficits in this clinically rather heterogeneous patient population.<sup>[2,23-25]</sup> From a practical clinical standpoint, our findings suggest that emphasis should be placed first and foremost on the specific brain regions involved by the neurodegenerative process,

and their functionality, as well as contribution to clinical symptomatology rather than left versus right sidedness of hypometabolism patterns.

### Limitations

Limitations of this study include a relatively small and heterogeneous dataset, retrospective nature, and limited availability of long-term patient follow-up to assess for morbidity and mortality, including potential clinical impact of left- versus right-sided predominant pathology. In addition, since many of our patients were referred by primary care physicians from the community, uniform neurologic and cognitive testing data are unfortunately lacking. In addition, while the primary diagnosis was used, it is well known that many dementia diagnoses include neurodegeneration across multiple domains of functioning and may reflect contemporaneous etiologies. To further elicit the potential clinical implications of these findings, follow-up brain PET/MRI is needed to fully characterize the progression of hypometabolism patterns, particularly in PPA patients. Furthermore, including functional MRI (fMRI) analyses to delineate the area and side of language dominance, tractography to assess for corresponding damage to white matter tracts as well as assessment of connectivity alterations within the language network using resting-state fMRI in future studies may help establish an underlying biologic basis for the described findings.

### CONCLUSION

Making an accurate neuroimaging diagnosis of neurodegenerative disease is becoming increasingly important, especially given the aging population and in the context of emerging dementia therapeutics. While prior reports in the literature strongly emphasize left-dominant patterns of hypometabolism in PPA patients, a third of our patients demonstrated right-sided dominant hypometabolism. Therefore, our findings emphasize the importance of assessing specific brain regions affected by neuronal demise and their functionality, rather than left versus right sidedness of metabolic deficits.

### Financial support and sponsorship

Nil.

### Conflicts of interest

There are no conflicts of interest.

### REFERENCES

- Arvanitakis Z, Shah RC, Bennett DA. Diagnosis and management of dementia: Review. *JAMA* 2019;322:1589-99.
- Olney NT, Spina S, Miller BL. Frontotemporal dementia. *Neurol Clin* 2017;35:339-74.
- Bonner MF, Ash S, Grossman M. The new classification of primary progressive aphasia into semantic, logopenic, or nonfluent/agrammatic variants. *Curr Neurol Neurosci Rep* 2010;10:484-90.
- Gorno-Tempini ML, Dronkers NF, Rankin KP, Ogar JM, Phengrasamy L, Rosen HJ, *et al.* Cognition and anatomy in three variants of primary progressive aphasia. *Ann Neurol* 2004;55:335-46.
- Gorno-Tempini ML, Hillis AE, Weintraub S, Kertesz A, Mendez M, Cappa SF, *et al.* Classification of primary progressive aphasia and its variants. *Neurology* 2011;76:1006-14.
- Baralle M, Buratti E, Baralle FE. The role of TDP-43 in the pathogenesis of ALS and FTLD. *Biochem Soc Trans* 2013;41:1536-40.
- Tsai RM, Bejanin A, Lesman-Segev O, LaJoie R, Visani A, Bourakova V, *et al.* 18F-flortaucipir (AV-1451) tau PET in frontotemporal dementia syndromes. *Alzheimers Res Ther* 2019;11:13.
- Cho H, Choi JY, Hwang MS, Kim YJ, Lee HM, Lee HS, *et al.* *In vivo* cortical spreading pattern of tau and amyloid in the Alzheimer disease spectrum. *Ann Neurol* 2016;80:247-58.
- James OG, Doraiswamy PM, Borges-Neto S. PET imaging of tau pathology in Alzheimer's disease and tauopathies. *Front Neurol* 2015;6:38.
- Josephs KA, Martin PR, Botha H, Schwarz CG, Duffy JR, Clark HM, *et al.* 18F]AV-1451 tau-PET and primary progressive aphasia. *Ann Neurol* 2018;83:599-611.
- Brown RK, Bohnen NI, Wong KK, Minoshima S, Frey KA. Brain PET in suspected dementia: Patterns of altered FDG metabolism. *Radiographics* 2014;34:684-701.
- Rosen HJ, Gorno-Tempini ML, Goldman WP, Perry RJ, Schuff N, Weiner M, *et al.* Patterns of brain atrophy in frontotemporal dementia and semantic dementia. *Neurology* 2002;58:198-208.
- Rabinovici GD, Jagust WJ, Furst AJ, Ogar JM, Racine CA, Mormino EC, *et al.* Abeta amyloid and glucose metabolism in three variants of primary progressive aphasia. *Ann Neurol* 2008;64:388-401.
- Matias-Guiu JA, Díaz-Álvarez J, Ayala JL, Risco-Martín JL, Moreno-Ramos T, Pytel V, *et al.* Clustering analysis of FDG-PET imaging in primary progressive aphasia. *Front Aging Neurosci* 2018;10:230.
- Josephs KA, Duffy JR, Fossett TR, Strand EA, Claassen DO, Whitwell JL, *et al.* Fluorodeoxyglucose F18 positron emission tomography in progressive apraxia of speech and primary progressive aphasia variants. *Arch Neurol* 2010;67:596-605.
- Madhavan A, Whitwell JL, Weigand SD, Duffy JR, Strand EA, Machulda MM, *et al.* FDG PET and MRI in logopenic primary progressive aphasia versus dementia of the Alzheimer's type. *PLoS One* 2013;8:e62471.
- Iaccarino L, Crespi C, Della Rosa PA, Catricalà E, Guidi L, Marcone A, *et al.* The semantic variant of primary progressive aphasia: Clinical and neuroimaging evidence in single subjects. *PLoS One* 2015;10:e0120197.
- Rascovsky K, Hodges JR, Knopman D, Mendez MF, Kramer JH, Neuhaus J, *et al.* Sensitivity of revised diagnostic criteria for the behavioural variant of frontotemporal dementia. *Brain* 2011;134:2456-77.
- Armstrong MJ, Litvan I, Lang AE, Bak TH, Bhatia KP, Borroni B, *et al.* Criteria for the diagnosis of corticobasal degeneration. *Neurology* 2013;80:496-503.
- Dickson DW, Bergeron C, Chin SS, Duyckaerts C, Horoupian D, Ikeda K, *et al.* Office of Rare Diseases neuropathologic criteria for corticobasal degeneration. *J Neuropathol Exp Neurol* 2002;61:935-46.
- Whitwell JL, Jack CR Jr, Boeve BF, Parisi JE, Ahlskog JE, Drubach DA, *et al.* Imaging correlates of pathology in corticobasal syndrome. *Neurology* 2010;75:1879-87.
- Bigio EH, Brown DF, White CL 3<sup>rd</sup>. Progressive supranuclear palsy with dementia: Cortical pathology. *J Neuropathol Exp Neurol* 1999;58:359-64.
- Höglinger GU, Respondek G, Stamelou M, Kurz C, Josephs KA, Lang AE, *et al.* Clinical diagnosis of progressive supranuclear palsy:

- The movement disorder society criteria. *Mov Disord* 2017;32:853-64.
24. Chen YJ, Dubroff, JG, Nasrallah IM. Recognizing common PET patterns in neurodegenerative dementia. *Appl Radiol* 2017;46:6-12.
  25. Rabinovici GD, Rosen HJ, Alkalay A, Kornak J, Furst AJ, Agarwal N, *et al.* FDG-PET in the differential diagnosis of AD and FTLN. *Neurology* 2011;77:2034-42.
  26. Cairns NJ, Bigio EH, Mackenzie IR, Neumann M, Lee VM, Hatanpaa KJ, *et al.* Neuropathologic diagnostic and nosologic criteria for frontotemporal lobar degeneration: Consensus of the consortium for frontotemporal lobar degeneration. *Acta Neuropathol (Berl)* 2007;114:5-22.
  27. Tsai RM, Boxer AL. Therapy and clinical trials in frontotemporal dementia: Past, present, and future. *J Neurochem* 2016;138:211-221.